Saudi Journal of Biological Sciences 27 (2020) 695–700

Contents lists available at ScienceDirect

Saudi Journal of Biological Sciences

journal homepage: www.sciencedirect.com

Original article

The construction of the scoliosis 3D finite element model and the biomechanical analysis of PVCR orthopaedy

Xuanhuang Chen [1], Hanhua Cai [1], Guodong Zhang [1], Feng Zheng, Changfu Wu, Haibin Lin *

Department of Orthopedics, The Affiliated Hospital of Putian University, Putian 351100, China

ARTICLE INFO

Article history:
Received 25 September 2019
Revised 13 November 2019
Accepted 3 December 2019
Available online 12 December 2019

Keywords:
Scoliosis
Stress
Model
Vertebral body
PVCR

ABSTRACT

Objective: The objective is to investigate the biomechanical conditions of the Posterior Vertebral Column Resection (PVCR) of the constructed scoliosis 3D finite element model.
Methods: A patient with scoliosis was selected; before the PVCR orthopaedy, the patient was submitted to the radiography of normal and lateral full-length vertebral column scans and the total magnetic resonance imaging (MRI) scans; then, the idiopathic scoliosis model was constructed by the 3D finite element method, and the 3D finite element software utilized in the process of model construction included Mimics software, Geomagic Studio 12 software, and Unigraphic 8.0 (UG 8.0) software; in addition, PVCR orthopaedy was utilized to correct the scoliosis of the patient, and the biomechanical parameters, such as orthodontic force, vertebral body displacement, orthopedic rod stress, stress on the pin-bone interface of the vertebral body surface, and the stress on the intervertebral disc, were studied.
Results: The 3D effective finite element model of scoliosis was successfully constructed by the Mimics software, the Geomagic Studio 12 software, and the UG 8.0 software, and the effectiveness was tested. PVCR orthopaedy could effectively solve the problem of scoliosis. The magnitude of the orthodontic force that a patient needed depended on the physical conditions and the personal orthodontic requirements of the patient. The maximum vertebral body displacement on the X-axis was the vertebral body L1, the maximum displacement on the Y-axis was the vertebral body T3, the maximum displacement on the Z-axis was the vertebral body T1, and the rang of orthopedic rod stress was $0.0050214e^7$ MPa to $0.045217e^7$ MPa, in which the maximum stress of 2 vertebral bodies in, above, and below the osteotomy area reached $0.045217e^7$ MPa, the stress on the pin-bone interface of the T10 vertebral body surface reached 11.83 MPa, and the stress of T8/T9 intervertebral disc reached 13.84 MPa.
Conclusion: The 3D finite element model based on 3D finite element software was highly efficient, and its numerical simulation was accurate, which was important for the subsequent biomechanical analysis of PVCR orthopaedy. In addition, the vertebral stress of PVCR orthopaedy was different in each body part, which was mainly affected by the applied orthodontic force and the sites of the orthodontic area.

1. Introduction

Scoliosis is a complex 3D planar deformity, which includes one or several segments of the vertebral column on the coronal plane that deviated from the median, thereby forming the lateral curvature; in addition, the physiological lordosis and kyphosis on the sagittal plane increase or decrease, and the rotational deformity of the vertebral column on the axial plane is seen (Wang et al., 2017; Ye et al., 2017; Liu et al., 2019). Scoliosis indicates the deformity of the torso, and the body shape of the patient is affected, resulting in the small and weak build of the patient who is accompanied by pains in the back and waist, and even symptoms of cardiac and pulmonary dysfunctions in severe cases (Shi et al., 2018). Severe scoliosis not only brings physical damages to the patient but also causes psychological obstacles to the patient, negative emotions to the families of the patient, and serious psychological trauma to both the patient and the families (Buckley et al., 2018). The effect of scoliosis on the quality of life and social and psychosocial conditions of the patient is obvious;

* Corresponding author.
E-mail address: binhai40207739@126.com (H. Lin).
[1] These authors contributed equally to this work as co-first author.
Peer review under responsibility of King Saud University.

Production and hosting by Elsevier

https://doi.org/10.1016/j.sjbs.2019.12.005
1319-562X/

therefore, scoliosis patient should be appropriately treated with appropriate surgical treatments (Cannestra et al., 2018). Since the beginning of the 1980s, the generation of instrument has made surgical vertebral column orthopaedy possible (however, the orthopaedy was the 2D orthopaedy-disconnection, the loss of orthopedic effects were common; especially, the incidence rate of postoperative flat back was high) (Richards, 2018; Ochsner's Tenth Annual Research, 2016); in addition to the subsequent generation and development of the vertebral screw and pin instrument, the orthopaedy of scoliosis truly entered the 3D orthopaedy era (Michelson, 2017).

As a result, the surgical treatments of scoliosis have entered a new phase and have been relatively mature. Severe rigid scoliosis can lead to the aggravation of pathological processes such as vertebral column injury and early degeneration. In severe cases, incomplete paralysis of the lower extremities may occur, or even complete paralysis (Clark and Bracci, 2019). Surgical treatment is the only solution and method; however, it is difficult and has high risks, and is prone to postoperative complications. Therefore, the intraoperative orthopedics must be comprehensively analyzed from the sagittal, axial, and coronal planes (Wang et al., 2016).

In summary, the biomechanical conditions of scoliosis PVCR orthopaedy of 3D finite element model were investigated. The results showed that the 3D finite element model was highly effective, which was important for the biomechanical analysis of PVCR orthopaedy. The stress of each vertebral body of a patient after PVCR orthopaedy was different and was largely affected by the orthodontic force and the sites of the orthodontic area. The innovation of the study lies in the detailed analysis and exploration of each stress and displacement of all involved vertebral bodies of the patient. The research results have provided certain guidance for future research, which is valuable.

2. Materials and methods

2.1. Research subject

Mr. Wang, a scoliosis patient who was admitted to a 3A hospital, was selected. The patient was 14 years old and weighed 50 kg. Before the operation, the full-length positive and lateral films of the patient's spine were taken, and the patient was examined by full-scale MRI to check the condition in the spinal canal. The patient was diagnosed as severe scoliosis. Prior to the trial, patients and their families signed the relevant informed consent, and the trial was approved by XXX ethics committee.

2.2. Construction of 3D finite element models of scoliosis

Import the CT images: First, the obtained data and CT images of vertebral column of the selected patient was imported to the Mimics 10.01 software where about 600 CT tomographic images were generated, with a distance of 0.5 mm between each slice; then, the images were submitted to the Mimics image processing software; it must ensure that no errors were in the front, back, top, and bottom biological positions of the images; the appropriate bone tissue gray value was selected, and the range was 0–3000.

Trim the scoliosis segment: The Remesh function carried in the FEA module of the Mimics image processing software was operated. First, the model needed basic cleaning and tidying. The problematic modules that appeared in the model needed to be sorted out to reduce the existence of excess problematic triangles. Mimics image processing software had already included the functions of "Grid re-division", "Model triangle editing", "Intersection triangle existence check", and "Smoothing model".

UG8.0 scoliosis model: In the previous step, the vertebral column models of the vertebral column, the pelvis, and other parts had been designed. Then, the 55 preliminary designs that had been processed by Geomagic Studio and Mimics 10.01 were imported to UG 8.0 software. By using the "stitching" function, it was possible to design the previous sheet module into a corresponding object.

Thoracic and lumbar vertebral segment assembly of the vertebral column: A total of 18 vertebral bodies including lumber vertebra T1-T6 and thoracic vertebra L1-L12 were defined as the core parts of the assembly. The angles between each surface and plane of each vertebral body on the sagittal and coronal planes were measured, and the length between the mutually connected vertebral bodies and the tapered holes were regarded as an important basis for assembly.

Further editing by UG 8.0: The vertebral column model divided the entire vertebra into 3 parts, i.e. the vertebral body, the vertebral arch, and the spinal cord and pedicle of vertebral arch in the middle. The thoracic vertebra was connected to the ribs from the first section of the vertebra, which was the important component of the thorax. The vertebral body was covered with a layer of hard bone cortex, while its internal was composed of loose and sponge-like spongy bones. The key section from the lumbar vertebra T2 to the vertebra was selected. The total number of intervertebral discs was 18. The nucleus and the annulus were assembled into a synthetic intervertebral disc. Based on the data research on the compositions of human body structure, the quality of the intact intervertebral disc was distributed in the ratio of nucleus pulposus to annulus fibrosus of 1:1.

Overall assembly of the vertebral column model: The previously completed vertebral body model was transferred to the UG 8.0 software in the format of the unified storage format such as the intervertebral disc and rib joints mentioned in previous steps. Based on the characteristics of the vertebral column of the vertebral body and the mutual relationship between the vertebral column and the vertebral body, the 3D finite element model required by the model was assembled. The technical flow chart was shown in Fig. 1.

2.3. PVCR biodynamical analysis

Real environment simulation: A board without any defects was selected to indicate the bed in the operation. The patient would be in a prone posture during the operation, and the operation position was on the back of the patient. According to the actual operation steps, the connected section of the thoracic bone and the pelvis were controlled; in terms of the model in operation simulation, it should be ensured that the skin of the pelvis must not contact with the bed during operation. In addition, the required activity between the vertebral body and the thorax must be ensured, and the lubrication of the articular capsule required a realistic simulation.

Orthopaedy simulation: Vertebral arch screw pin placement and rod placement. The commands such as "Spatial curve" and "Stretching resection" of the UG 8.0 software were utilized to construct the 3D model of the orthodontic screw pin. After several attempts, each titanium alloy orthodontic screw pin was accurately implanted in UG 8.0 software. In addition, the titanium alloy orthodontic rods needed in the operation was generated by using the "Scanner", "Spatial curve", and "Boolean difference" commands at the tail of each screw pin.

Vertebral resection and application of orthopedic force: In PVCR orthopaedy, it was necessary to apply an orthopedic force to exert force on the vertebral column of a patient who had been equipped with pin-rod orthodontic devices so that the vertebral bodies that

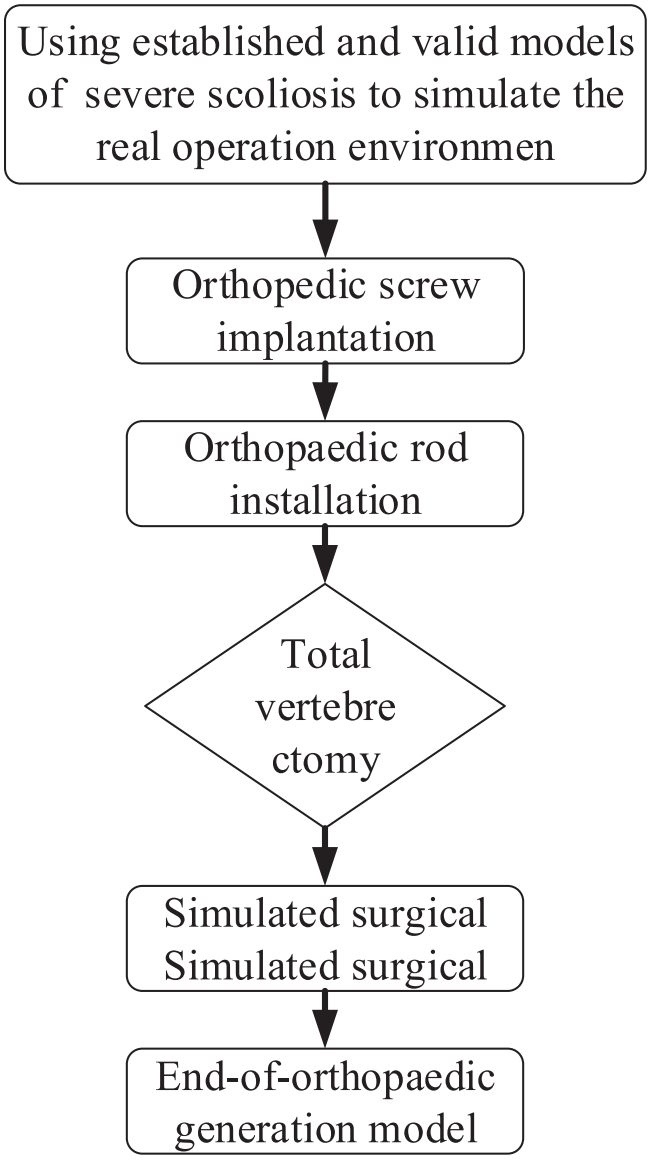

Fig. 1. The road map of assembly technology.

were originally in offset states were restored to the normal spatial range of the vertebral column and vertebral body of a healthy human body as much as possible. In addition, the force line of the vertebral column was restored so that the vertebral column of the patient after orthopedic would conform to the aesthetic of normal human anatomy. The simulated orthopedic force was as follows: relation setting of the thoracic, pelvic, and body position to the operation bed, and the relation setting between the articular capsules.

2.4. Statistics analysis

The measured values and obtained data were input into the statistical software SPSS 19.0 for T-test to determine the presence or absence of significant differences between the assembled model in the UG and the actual conditions of the patient. The difference standard is the average stiffness value in six directions after loading 4N.M moment in T1-T4 of thoracic vertebrae; the angle deviation in six directions after loading 4N.M moment in T1-T4 of thoracic vertebrae; the stress of disc in T8/T9 position after PVCR; the stress of orthopedic rod after PVCR; the maximum stress distribution of screw bone interface on the screw surface of each vertebrae after PVCR; the maximum movement of each vertebral body on Z axis after PVCR.

During and after PCVR, the displacement of each vertebral body, pedicle, screw, rod, screw rod joint, screw bone interface, disc stress, and deviation angle were input into the statistical database. If the differences were found, the assembly needed to be adjusted according to the above table; otherwise, the other tests were continued.

3. Results and discussion

3.1. Effectiveness test of the stiffness of scoliosis 3D finite element models

The analysis of the mean stiffness value in 6 directions after the loading of 4N.M force moment to thoracic vertebra T1-T4 was shown in Fig. 2. As can be seen from the figure, after the loading of 4N.M force moment to thoracic vertebra T1-T4, the stiffness values obtained through the constructed 3D finite element model in any directions such as anteflexion, retroflexion, left-deviation, right-deviation, left-rotation, and right-rotation were very close to those obtained by Panjabi and Busschr that were already well-accepted with very small deviations. Therefore, the constructed 3D finite element model of scoliosis was effective.

3.2. Effectiveness test of the angle offset of scoliosis 3D finite element models

The analysis of the angle offset in 6 directions after the loading of 4N.M force moment to thoracic vertebra T1-T4 was shown in Fig. 3. As can be seen from the figure, after the loading of 4N.M force moment to thoracic vertebra T1-T4, the angle offset obtained through the constructed 3D finite element model in any directions such as anteflexion, retroflexion, left-deviation, right-deviation, left-rotation, and right-rotation was very close to those obtained by Panjabi that were already well-accepted with very small deviations. Therefore, the constructed 3D finite element model of scoliosis was effective.

3.3. Stress analysis of each intervertebral disc after PVCR orthopaedy

The analysis of the maximum stress of each intervertebral disc after PVCR orthopaedy was shown in Fig. 4. As can be clearly seen from the figure, the maximum stress of T8/T9 intervertebral discs after PVCR orthopaedy reached 14 MPa, while the minimum stress was found at T5/T6 and T6/T7 intervertebral discs, which was 3 MPa. During the orthopaedy, the applied orthopedic force must be comprehensively considered based on the physical conditions, age, bone mineral density, gender, etc. of each patient instead of blindly pursuing the beauty to ensure that after the orthopaedy, the outcomes were acceptable to the patient both physically and mentally, and the irreparable sequelae must be avoided.

3.4. Stress analysis of orthopedic rods after PVCR orthopaedy

The stress analysis of orthopedic rods after PVCR orthopaedy was shown in Fig. 5. As can be seen from the figure, the maximum stress of the orthopedic rod lied in the 2 vertebral bodies above and below the osteotomy area; therefore, after the PVCR orthopaedy, the probability of the orthopedic rod fracture in the osteotomy area was the highest. Studies have shown that in the orthopedic rod fractures, 21% of the orthopedic rods broke at the position of the osteotomy area; thus, in order to reduce the occurrence of frac-

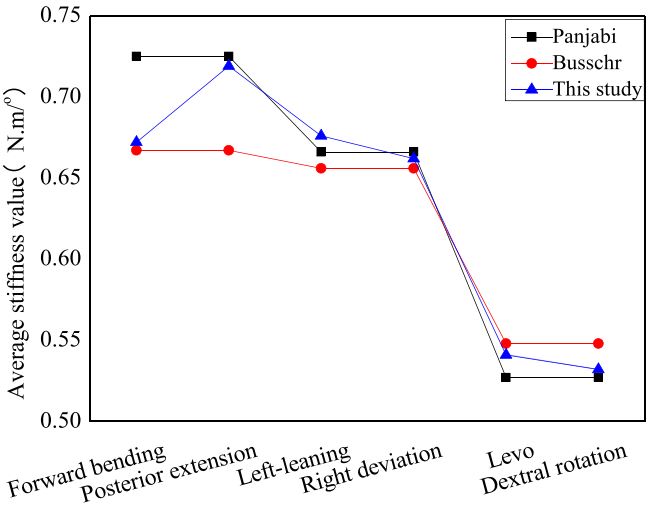

Fig. 2. Analysis of the mean stiffness value in 6 directions after the loading of 4N.M force moment to thoracic vertebra T1-T4.

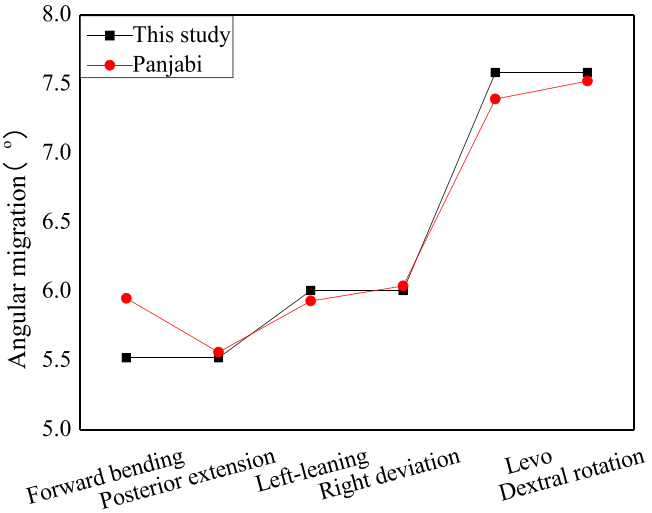

Fig. 3. Analysis of the angle offset in 6 directions after the loading of 4N.M force moment to thoracic vertebra T1-T4.

tures in the orthopedic rods, it was necessary to utilize multiple orthopedic rods in the postoperative osteotomy area to maximize the occurrence and the negative effects of fractures.

3.5. Stress analysis of each pin-bone interface after PVCR orthopaedy

The analysis of the maximum stress distribution on the pin-bone interface on the surface of each vertebral screw pin after PVCR orthopaedy was shown in Fig. 6. As can be seen from the figure, after the PVCR orthopaedy, the pin-bone stress on each vertebral body surface was affected by the orthopedic screw pins, thereby the possibility of vertebral body fractures was extremely high, as well as the possibility of the screw pin fractures. The stresses that occurred at the site where the vertebral body of the patient and the screw pins were connected were generally the largest. At the same time, it could be seen from the analysis of the maximum stress of each vertebral body that in the PVCR orthopaedy, compared with the stress of other vertebral bodies, the stress of T9 and T10 vertebral bodies were much higher and were closely related to the orthopedic area.

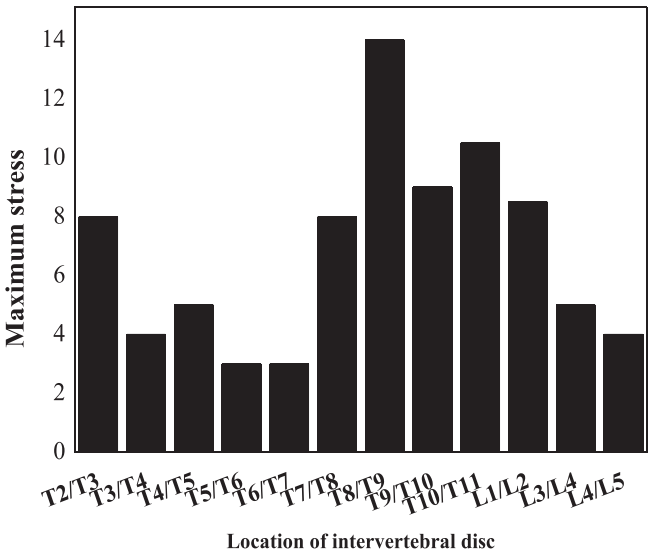

Fig. 4. Analysis of the maximum stress of each intervertebral disc after PVCR orthopaedy.

3.6. Analysis of major vertebral body movements after PVCR orthopaedy

The maximum movement of each vertebral body on the Z-axis after PVCR orthopaedy was shown in Fig. 7. As can be clearly seen from the figure, the maximum movement of T1 vertebral body after PVCR orthopaedy reached 32, while the minimum movement on the Z-axis was found in T5 vertebral body, which was 5. During the orthopaedy, the applied orthopedic force must be comprehensively considered based on the physical conditions, age, bone mineral density, gender, etc. of each patient instead of blindly pursuing the beauty to ensure that after the orthopaedy, the outcomes were acceptable to the patient both physically and mentally, and the behaviors that may bring greater risks to the patient must be avoided.

4. Discussion

The biomechanical conditions of PVCR orthopaedy of the constructed scoliosis3D finite element model were investigated. A patient with scoliosis was selected; before the PVCR orthopaedy, the patient was submitted to the radiography of normal and lateral full-length vertebral column scans and the total MRI scans; then, the idiopathic scoliosis model was constructed by the 3D finite element method, and the 3D finite element software utilized in the process of model construction included Mimics software, Geomagic Studio 12 software, and UG 8.0 software; in addition, PVCR orthopaedy was utilized to correct the scoliosis of the patient, and the biomechanical parameters, such as orthodontic force, vertebral body displacement, orthopedic rod stress, stress on the pin-bone interface of the vertebral body surface, and the stress on the intervertebral disc, were studied (Liu et al., 2017). The results showed that the 3D effective finite element model of scoliosis was successfully constructed by the Mimics software, the Geomagic Studio 12 software, and the UG 8.0 software, and the effectiveness was tested. PVCR orthopaedy could effectively solve the problem of scoliosis (Cobetto et al., 2016). The magnitude of PVCR orthodontic force that a patient needed depended on the physical conditions and the personal orthodontic requirements of the patient (Henao et al., 2016). The maximum vertebral body displacement on the

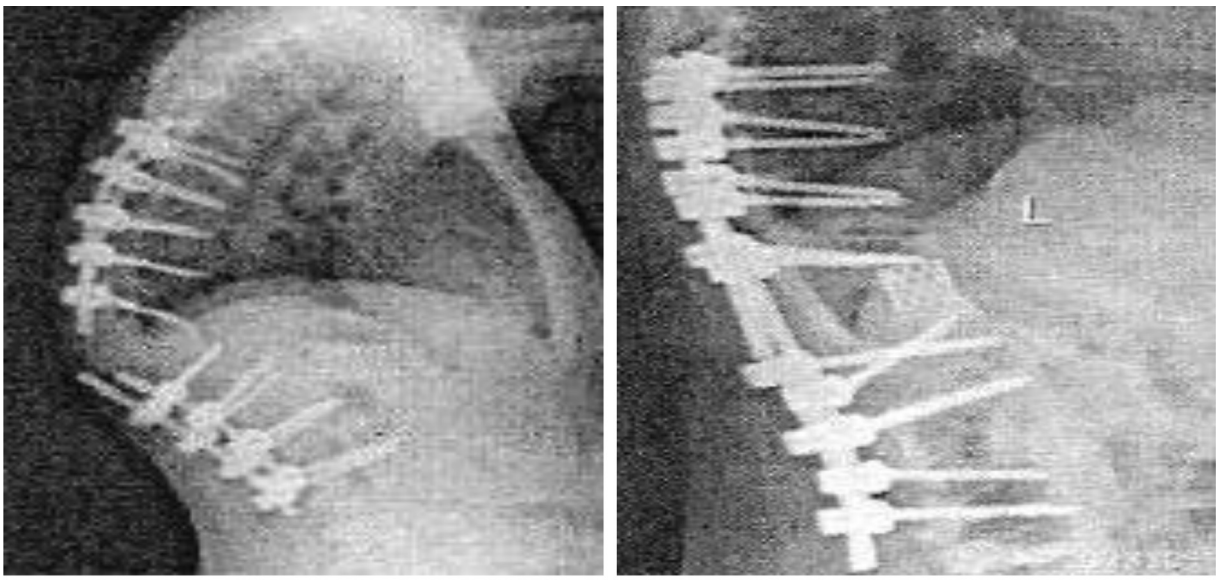

Fig. 5. Stress analysis of orthopedic rods after PVCR orthopaedy.

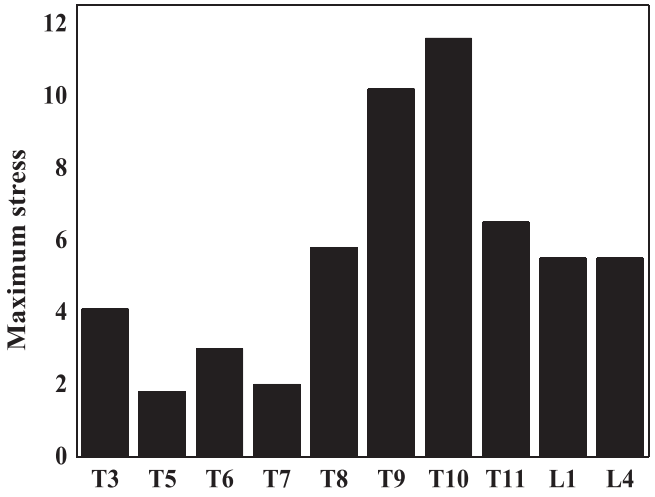

Fig. 6. Analysis of the maximum stress distribution on the pin-bone interface on the surface of each vertebral screw pin after PVCR orthopaedy.

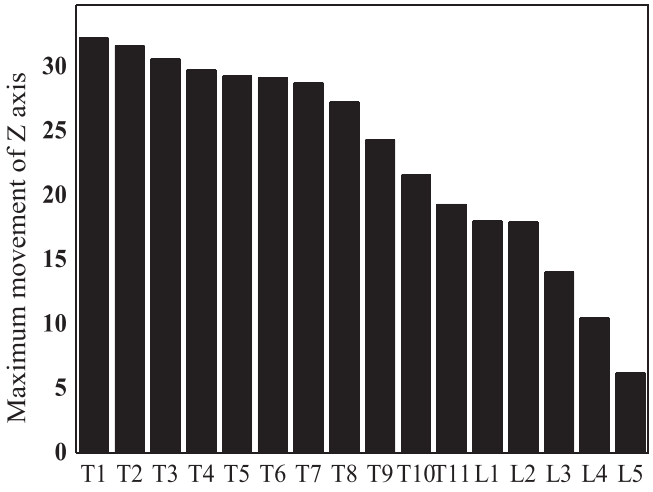

Fig. 7. The maximum movement of each vertebral body on the Z-axis after PVCR orthopaedy.

X-axis was the vertebral body L1, the maximum displacement on the Y-axis was the vertebral body T3, the maximum displacement on the Z-axis was the vertebral body T1, and the rang of orthopedic rod stress was 0.0050214e^7 MPa to 0.045217e^7 MPa, in which the maximum stress of 2 vertebral bodies in, above, and below the osteotomy area reached 0.045217e^7 MPa, the stress on the pin-bone interface of the T10 vertebral body surface reached 11.83 MPa, and the stress of T8/T9 intervertebral disc reached 13.84 MPa. Thus, it was concluded that the 3D finite element model was effective, the therapeutic effect of PVCR orthopaedy on scoliosis patient was significant, and the magnitude of vertebral body stress of the patient was affected by the orthodontic force and the sites of the orthodontic area. Age, gender, bone maturity, osteoporosis and so on could affect the pullout strength of screws. The results of this study suggested that with the increase of orthopedic strength, intraoperative fracture of vertebral body and failure of endophyte could be directly caused. However, the specific amount of load applied during the operation should be determined according to the patient's actual situation, age, gender, bone density, etc. It was necessary to take the strength to make the patients achieve the ideal orthopedic effect. In the pursuit of perfect orthopedic effect, reasonable control of orthopedic strength could greatly reduce the failure of internal fixation.

Therefore, the biomechanical conditions of scoliosis PVCR orthopaedy were analyzed through the construction of 3D finite element model and the simulation of PVCR orthopaedy; it was found that PVCR orthopaedy could effectively improve the physical conditions of patients with scoliosis, and the 3D finite element model and PVCR orthopaedy-centered intervention treatment had important research value. However, certain limitations were also found in the research. For example, when the PVCR technique was presented, the process cannot be displayed in a dynamic form, and only the static results can be selected; in addition, the effects of muscle on the results were ignored during the model construction. Despite the deficiencies, the research has important reference value for subsequent studies.

Fund project

Fujian province clinical key specialty construction project (2018145); Fujian province Putian city clinical key specialty construction project (2016228); Science and Technology Project of Putian City of Fujian Province, No. 2018S3F003.

Declaration of Competing Interest

The authors declared that there is no conflict of interest.

References

Buckley, C.T., Hoyland, J.A., Fujii, K., et al., 2018. Critical aspects and challenges for intervertebral disc repair and regeneration—harnessing advances in tissue engineering. JOR Spine 1 (3), 1029.

Cannestra, A., Schroerlucke, S., Wang, M., et al., 2018. Best paper session A001: complications and revision rates in robotic-guided vs fluoro-guided minimally invasive lumbar fusion surgery – a report from the mis refresh prospective. Global Spine J. 8 (1), 2–173.

Clark, M., Bracci, E., 2019. Serotonergic modulation of the ventral pallidum by 5HT1A, 5HT5A, 5HT7 AND 5HT2C receptors. Brain Neurosci. Adv. 3, 229–230.

Cobetto, N., Aubin, C.E., Parent, S., et al., 2016. Effectiveness of braces designed using computer-aided design and manufacturing (CAD/CAM) and finite element simulation compared to CAD/CAM only for the conservative treatment of adolescent idiopathic scoliosis: a prospective randomized controlled trial. Eur. Spine J. 25 (10), 3056–3064.

Henao, J., Aubin, C.É., Labelle, H., et al., 2016. Patient-specific finite element model of the spine and spinal cord to assess the neurological impact of scoliosis correction: preliminary application on two cases with and without intraoperative neurological complications. Comput. Methods Biomech. Biomed. Eng. 19 (8), 901–910.

Liu, X., Ma, J., Park, P., et al., 2017. Biomechanical comparison of multilevel lateral interbody fusion with and without supplementary instrumentation: a three-dimensional finite element study. BMC Musculoskeletal Disorders 18 (1), 63.

Liu, Y., Zhou, G., Xu, N., 2019. Biomechanical evaluation of osteoporosis treating with mechanical vibrations: a finite element analysis. Nanosci. Nanotechnol. Lett. 11 (4), 506–513.

Michelson, D.J., 2017. Spinal fluid examination. Swaiman's Pediatric Neurology E-Book: Principles Practice 1 (2), 160.

Ochsner's Tenth Annual Research Day May 17, 2016 Ochsner Clinic Foundation New Orleans, LA, Ochsner J. 16 (2016) 337–424.

Richards, B., 2018. Bone research society, annual meeting 2017 proceedings. J. Musculoskelet Neuronal Interact 18 (1), 108–151.

Shi, B., Xu, L., Mao, S., et al., 2018. Abnormal PITX1 gene methylation in adolescent idiopathic scoliosis: a pilot study. BMC Musculoskeletal Disorders 19 (1), 138.

Wang, Z., Chen, H., Yu, Y.E., et al., 2017. Unique local bone tissue characteristics in iliac crest bone biopsy from adolescent idiopathic scoliosis with severe spinal deformity. Sci. Rep. 7, 40265.

Wang, L., Zhang, B., Chen, S., et al., 2016. A validated finite element analysis of facet joint stress in degenerative lumbar scoliosis. World Neurosurgery 95, 126–133.

Ye, J., Liu, B., Liu, J., et al., 2017. Research on electrical measurement experiment of deformation of artificial thorax model. J. Mech. Med. Biol. 17 (03), 1750057.